The Added Value of ^{18}F-FDG PET/CT for Evaluation of Patients with Esthesioneuroblastoma

Stephen M. Broski[1], Christopher H. Hunt[1], Geoffrey B. Johnson[1], Ratham M. Subramaniam[2], and Patrick J. Peller[1]

[1]*Department of Radiology, Mayo Clinic, Rochester, Minnesota; and* [2]*Department of Radiology, Boston University Medical Center, Boston, Massachusetts*

The purpose of this study was to evaluate the clinical utility of ^{18}F-FDG PET/CT in esthesioneuroblastoma staging and restaging and quantify the additional benefit of PET/CT to conventional imaging. **Methods:** A retrospective review was performed with institutional review board approval for patients with a diagnosis of esthesioneuroblastoma who underwent PET/CT from 2000 to 2010. PET/CT results were retrospectively reviewed by *2* radiologists who were unaware of the clinical and imaging data. Positive imaging findings were classified into 3 categories: local disease, cervical nodal spread, and distant metastasis. All conventional imaging performed in the 6 mo preceding PET/CT, and the medical records, were reviewed to determine the potential added value. **Results:** Twenty-eight patients (mean age, 52.3 ± 10 y; range, 23–81 y) were identified who underwent a total of 77 PET/CT examinations. Maximum standardized uptake value (SUVmax) was 8.68 ± 4.75 (range, 3.6–23.3) for the primary tumor and 8.57 ± 6.46 (range, 1.9–27.2) for the metastatic site. There was no clear association between primary tumor SUVmax and tumor grade ($P = 0.30$). Compared with conventional imaging, PET/CT changed disease stage or altered clinical management in 11 (39%) of 28 esthesioneuroblastoma patients. Of these, 10 (36%) of 28 were upstaged on the basis of their PET/CT studies. Cervical nodal metastases were found in 5 (18%) of 28, local recurrence in 2 (7%) of 28, cervical nodal and distant metastases in 2 (7%) of 28, and distant metastases in 1 (4%) of 28. One patient (4%) was downstaged after negative findings on PET/CT. **Conclusion:** PET/CT is a useful adjunct to conventional imaging in the initial staging and restaging of esthesioneuroblastoma by detecting nodal and distant metastatic disease not demonstrated by conventional imaging and identifying local recurrence hidden by treatment changes on conventional imaging.

Key Words: esthesioneuroblastoma; PET/CT; olfactory neuroblastoma

J Nucl Med 2012; 53:1200–1206
DOI: 10.2967/jnumed.112.102897

Esthesioneuroblastoma, also known as olfactory neuroblastoma, is an uncommon neuroendocrine tumor believed to arise from olfactory epithelium high in the nasal cavity. Although often insidious in onset, this tumor is locally aggressive and frequently recurs, with a tendency to involve the paranasal sinuses, orbit, and anterior cranial fossa (*1–3*). Regional metastases occur most commonly to cervical lymph nodes, and it is well documented that cervical nodal metastasis is one of the most important prognostic factors in survival (*4*). The overall incidence of cervical lymph node metastasis is between 20% and 25%, but approximately only 5% of patients present with positive nodal disease, signifying the tendency toward delayed nodal metastasis (*5*). Distant metastasis to bone, liver, and lung occurs less commonly and also frequently is delayed (*1–3*). Kadish et al. first proposed an A–C staging classification for esthesioneuroblastoma based on paranasal sinus involvement (*3*), which was subsequently modified to establish a group D for tumors with cervical lymph node or distant metastases (Table 1) (*6*). This staging system has been validated in several studies and was shown to correlate with survival (*4,7*).

^{18}F-FDG PET/CT has proven to be a useful adjunct to conventional imaging in more common malignancies, leading to improved pretreatment staging, assessment of treatment response, and differentiation of early recurrence from therapy-induced changes. To date, MRI and CT have been the primary imaging modalities used for evaluation of patients with esthesioneuroblastoma (*8–11*). Limited research has been performed on the role of ^{18}F-FDG PET/CT in esthesioneuroblastoma (*12*); the largest series to date included 12 patients having undergone PET/CT, and the modality was deemed appropriate for detecting cervical metastasis given their propensity for ^{18}F-FDG avidity (*8*). Therefore, our aim was to evaluate the clinical utility of ^{18}F-FDG PET in the diagnosis, staging, and restaging of esthesioneuroblastoma and to quantify the potential additional benefit of PET/CT to conventional imaging.

MATERIALS AND METHODS

After obtaining institutional review board approval, we performed a retrospective review of our institutional database for patients with a PET/CT study and the diagnosis of esthesioneuroblastoma from 2000 to 2010. The pathologic diagnosis of esthesioneuroblastoma was confirmed in all cases. The modified Kadish staging system was used for all patients on the basis of pathologic findings at subsequent biopsy or operative resection.

Received Jan. 11, 2012; revision accepted Mar. 15, 2012.
For correspondence or reprints contact: Stephen M. Broski, Mayo Clinic, Mayo Building, E2, 200 First St., SW, Rochester, MN 55905.
E-mail: Broski.stephen@mayo.edu
Published online Jun. 22, 2012.

TABLE 1
Modified Kadish Staging System

Stage	Description
A	Tumor confined to nasal cavity
B	Tumor confined to nasal cavity and paranasal sinuses
C	Tumor extent beyond nasal cavity and paranasal sinuses, including involvement of cribriform plate, base of skull, orbits, and intracranial cavity
D	Tumor with metastasis to cervical lymph nodes or distant site

Adapted from Kadish et al. (*3*) and Morita et al. (*6*).

All PET/CT studies (Discovery LS, RX, or 690; GE Healthcare) were performed according to the institutional standard clinical protocol. Weight, height, and blood glucose levels were recorded for all patients. All patients had a blood glucose level of less than 200 mg/dL, and all patients were injected with 444–629 MBq (12–17 mCi) of ^{18}F-FDG, with an incubation period of approximately 60 min. The ^{18}F-FDG dosage generally decreased over the 10-y study period; higher amounts (555–629 MBq [15–17 mCi]) were used during earlier studies. The amount of injected radioactivity was routinely measured by quantifying the radioactivity of the syringe before and after injection. Patients were imaged with arms up, from orbits to mid thigh (in 3 dimensions, using a 128 × 128 matrix and a rate of 3 min per bed position), and then dedicated head-and-neck images were acquired with the arms down (in 3 dimensions, using a 256 × 256 matrix and a rate of 5 min per bed position). PET images were reconstructed with a 3-dimensional ordered-subsets expectation maximization algorithm (28 subsets, 2 iterations). Low-dose helical CT images were obtained for attenuation correction and anatomic localization (detector row configuration, 16 × 0.625 mm; pitch, 1.75; gantry rotation time, 0.5 s; slice thickness, 3.75 mm; 140 kVP; and a range of 60–120 mAs using automatic current-modulation).

All PET/CT images were analyzed using an Osirix 3.3.2-DICOM viewer for Mac OS X (Apple). Initial review was performed by a diagnostic radiology resident with 8 y of PET/CT experience, and consensus was reached after separate analysis by a radiologist with both neuroradiology and nuclear medicine fellowship training, board certification in neurology, and 7 y of clinical experience. The pattern of ^{18}F-FDG uptake and degree of ^{18}F-FDG accumulation within the primary tumor, locoregional lymph nodes, and distant metastatic sites were recorded. PET/CT findings were considered positive if they demonstrated lesions with qualitatively increased uptake as compared with the adjacent blood pool. A quantitative standardized uptake value threshold was not used. The maximum standardized uptake value (SUVmax) was determined by visually identifying the region or regions on the PET images that qualitatively appeared to have the most intense ^{18}F-FDG uptake. A region of interest incorporating the gross tumor or metastasis volume was identified by the radiologist for SUVmax determination. Positive imaging findings were classified into 3 categories: local disease, cervical lymph node spread, and distant metastasis. The location of cervical lymph nodes was assigned according to the standard 7-level scheme (*13*).

All images and interpretations from conventional imaging (including MRI, CT, and sonography) performed in the 6 mo before each PET/CT study were analyzed. Concordance was noted between PET/CT and conventional imaging–reported local recurrence, cervical nodal metastasis, and distant metastasis. Because some patients underwent multiple PET/CT examinations over the 10-y period, and multiple conventional imaging examinations sometimes occurred over the 6 mo preceding each PET/CT study, each comparison between PET/CT and each individual conventional imaging examination was treated as a unique evaluation. All imaging findings were compared with histopathologic reports and clinical notes in the same 6-mo period. PET/CT interpretations were divided into true-positive, false-negative, false-positive, and true-negative, and PET/CT interpretations that were discordant with conventional imaging or histopathologic reports were noted. A thorough review of each patient's record was then undertaken to determine the clinical impact of the discordant PET/CT interpretation on management.

RESULTS

Twenty-eight patients were identified who underwent a total of 77 PET/CT examinations. Eleven (39%) were female, and 17 (61%) were male. The mean age was 52.3 ± 10 y, and the range was 23–81 y. Eleven patients (39%) underwent PET/CT for staging, and the remaining 17 patients (61%) underwent PET/CT for restaging or surveillance. Pathologic grade based on the Hyams scale was available for 19 of the 28 patients, 10 of whom had low-grade disease (Hyams I–II) and 9 high-grade (Hyams III–IV). Using the modified Kadish system, 4 (14%) of 28 patients were classified as having stage B disease, 10 (36%) of 28 as having stage C, and 14 (50%) of 28 as having stage D (Table 2).

Local recurrence, either within the nasal cavity, within adjacent paranasal sinuses, or intracranially, occurred in 10 (59%) of 17 patients and was the only site of recurrence in 6 (35%) of 17 patients. Fourteen (50%) of 28 patients had cervical lymph node disease. Only 4 (14%) of 28 had distant metastatic disease, which included the axial and appendicular skeleton, mediastinal and hilar lymph nodes, lung, and cervical epidural space, as well as diffuse leptomeningeal involvement.

The SUVmax for primary esthesioneuroblastoma sites, including both primary tumor and primary site recurrence (11 patients total), was 8.68 ± 4.75 with a range of 3.6–23.3. The SUVmax for all metastatic sites, including cervical lymph nodes and distant metastases (13 patients total), was 8.57 ± 6.46 with a range of 1.9–27.2. There was no statistically significant association between SUVmax of

TABLE 2
Patient Demographics

Characteristic	Value
Age (y)	
Mean	52.3 ± 10
Range	23–81
Sex (*n*)	
Male	11 (39%)
Female	17 (61%)
PET/CT indication (*n*)	
Staging	11 (39%)
Restaging	17 (61%)
Hyams pathologic grade (*n*)	
No grade	9 (32%)
Low grade (I–II)	10 (36%)
High grade (III–IV)	9 (32%)
Modified Kadish stage (*n*)	
Stage A	0 (0%)
Stage B	4 (14%)
Stage C	10 (36%)
Stage D	14 (50%)

the primary esthesioneuroblastoma site and tumor grade ($P = 0.30$, Kruskal-Wallis 1-way ANOVA).

There were a total of 85 conventional imaging studies (17 CT, 63 MRI, and 5 sonography) performed for the diagnosis or surveillance of esthesioneuroblastoma in the 6 mo preceding each PET/CT study; there were often differences in the conventional imaging that each patient received, as imaging was dictated by ordering clinician preference. Of the 77 PET/CT examinations, 22 (29%) exhibited discrepancy when compared with conventional imaging studies. Fourteen patients (50%) accounted for these 22 PET/CT examinations. Because some PET/CT studies had more than 1 comparison conventional imaging study, there were 33 total discordant instances, most of which (29/33) occurred in comparison with MRI (Table 3).

Ten (36%) of 28 patients were upstaged according to the Kadish system, on the basis of their PET/CT studies. All true-positive PET/CT findings were determined to be so on the basis of pathologic confirmation by subsequent biopsy or surgical resection. This included 5 (18%) of 28 patients in whom new cervical metastatic disease was discovered that was missed on MRI (Fig. 1). Four of these patients had undergone PET/CT for restaging or surveillance, and the other for staging. Of these 5 patients, 4 (14%) underwent neck dissection as a result of their PET/CT examinations. The management of the other patient was not changed; that patient received systemic chemotherapy given the extent of the primary tumor. Two (7%) of 28 patients underwent PET/CT that demonstrated local recurrence, whereas the corresponding MRI study was interpreted as showing postoperative change (Fig. 2). One of these patients received γ-radiotherapy to the recurrent region, whereas the other was treated conservatively with close observation. Two (7%) of 28 patients were found to have both metastatic cervical nodes and distant osseous metastases. The treatment approach for one of these patients was changed from potential surgical resection to salvage chemotherapy, whereas the other patient was treated conservatively. An additional patient (4%) was found to have new extensive osseous metastases, which were treated with palliative radiation therapy (Fig. 3).

Five (18%) of 28 patients underwent PET/CT that proved to be false-negative, on the basis of pathologic confirmation in 4 patients and progression on clinical follow-up imaging in 1 patient. Three of these patients had intracranial metastases that were missed by PET/CT (Fig. 4). The other 2 patients had mild or no ^{18}F-FDG uptake in a locally recurrent tumor, which was interpreted as postoperative inflammatory changes or no recurrence on PET/CT (Fig. 5). All were managed with surgical resection, radiation therapy, or a combination of both based on the MRI examinations (Table 3).

One patient (4%) of 28 had a PET/CT finding of an ^{18}F-FDG–avid cervical lymph node, which was reactive on biopsy and proved to be false-positive. The PET/CT results of an additional patient (4%) were read as negative, whereas the comparison MRI was interpreted to be positive for locally recurrent esthesioneuroblastoma. The patient was managed with close observation, and subsequent studies over an 8-y period demonstrated no evidence of recurrence, after which the patient was managed elsewhere. PET/CT was considered to be true-negative in that instance.

DISCUSSION

Esthesioneuroblastoma is an insidious tumor, which is often quite advanced at initial presentation and has a propensity for local recurrence and late distant metastases (*1–3*). Stage at initial presentation is highly predictive of survival; therefore, accurate staging is essential. The tendency toward late metastasis necessitates continued long-term surveillance (*14*). For these reasons, imaging is critical for medical management of patients with esthesioneuroblastoma. Although the standard primary treatment for patients with nonmetastatic esthesioneuroblastoma is craniofacial resection and adjuvant radiation therapy, neoadjuvant or adjuvant chemotherapy is often added in patients with more advanced disease, in particular Kadish stage C (*15*). Neck dissection and radiotherapy are reserved for patients with evident neck nodal metastases (*5*). Even patients with late cervical lymph node metastases can be treated with acceptable salvage rates (*5,15,16*). Salvage therapy in esthesioneuroblastoma with delayed nodal spread was analyzed in several studies, the largest of which demonstrated an approximately 30% successful 1-y salvage rate of late neck metastases with surgery, radiation, or combined therapy (*16*). By more accurately delineating local tumor extent and elucidating cervical and distant metastases, PET/CT can inform these therapeutic decisions.

In our study, the additional information provided by PET/CT changed the disease stage or altered clinical management in 11 (39%) of 28 esthesioneuroblastoma

TABLE 3
Discordant PET/CT and Conventional Imaging Findings

Patient no.	Age (y)	Sex	Kadish stage at time of examination	PET/CT	Number/type conventional imaging	Anatomic site of discordance	Clinical impact
1	50	M	D	Restaging	2 MRI	Levels I and II	TP, bilateral radical neck dissection
2	5	F	D	Restaging	1 MRI	Level I	TP, selective neck dissection
3	5	F	D	Restaging	1 MRI/1CT	Level I	TP, selective neck dissection
4	46	M	D	Restaging	1 MRI	Levels I, II, III, and IV, RPLN	TP, bilateral modified neck dissection
4	47	M	D	Restaging	1 MRI	R PPF	TP, γ-knife therapy
5	66	F	D	Restaging	2 MRI	Level II/lumbar epidural	TP, prompted LN Bx; palliative spinal XRT given carcinomatosis
6	44	F	D	Restaging	1 MRI	Distant osseous	TP, palliative radiation
6	45	F	D	Restaging	1 MRI	Distant osseous	TP, palliative radiation
6	44	F	D	Restaging	1 MRI	Distant osseous	TP, prompted bone Bx; treatment changed to salvage chemotherapy
7	44	M	C	Staging	1 MRI/1 CT	Level II	TP, systemic chemotherapy given stage C primary
7	44	M	D	Restaging	2 MRI	Level II	TP, prompted Bx; neoadjuvant chemotherapy
8	70	M	D	Restaging	3 MRI	Maxillary sinus	TP, prompted Bx; conservative management
9	42	M	D	Restaging	1 CT	Level I/distant osseous	TP, conservative management
4	48	M	D	Restaging	2 MRI	L PPF/infraclavicular LN	TP, palliative care
10	80	F	D	Restaging	1 MRI	ACF	FN, therapy based on MRI
10	81	F	D	Restaging	2 MRI	ACF	FN, therapy based on MRI
11	37	F	C	Restaging	1 CT/1 MRI	ACF	FN, therapy based on MRI
12	48	M	C	Restaging	2 MRI	Frontal/parietal dura	FN, therapy based on MRI
4	47	M	D	Restaging	1 MRI	Ethmoid sinus	FN, therapy based on MRI
13	40	F	B	Restaging	1 MRI	L sphenoid/ethmoid	FN, therapy based on MRI
14	50	M	C	Staging	1 MRI	Level III	FP, pathology showed reactive node
14	50	M	C	Restaging	1 MRI	Cribriform plate/ACF	TN, MRI false-positive; no recurrence to date

TP = true-positive; RPLN = retropharyngeal lymph node; PPF = pterygopalatine fossa; LN = lymph node; Bx = biopsy; XRT = radiation therapy; ACF= anterior cranial fossa; FN = false-negative; FP = false-positive; TN = true-negative.

patients. Of these patients, 5 (18%) of 28 were found to have cervical nodal metastases by PET/CT that were either missed on MRI or CT or were otherwise unknown. The discovery of cervical metastases significantly altered clinical management, as 4 of these 5 patients underwent radical, modified radical, or selective neck dissection. Two patients (7%) of 28 were found to have local recurrence that was missed on MRI, one of which underwent stereotactic radiotherapy. One patient's planned treatment was changed from surgical resection and adjuvant radiation therapy of local recurrence to salvage chemotherapy given the burden of disease demonstrated on PET/CT.

The addition of PET/CT conferred an advantage over MRI alone for several reasons. Brain or facial MR images were obtained in most esthesioneuroblastoma patients, with axial acquisition extending inferiorly to the angle of the mandible. As such, cervical lymph nodes were seldom included in the field of view, and if they were, often only the most superior nodal levels were included. If level I or II nodes were included, they were often visualized on the last image slices, where they were more prone to be overlooked. Often dedicated neck MRI examinations were obtained only in patients with prior cervical nodal metastases or with a strong clinical suspicion of cervical nodal involvement. In esthesioneuroblastoma patients, whole-body PET/CT offers a wide field of view extending from the orbits to the mid thigh, which encompasses regions of possible local recurrence, cervical nodal metastasis, and distant metastasis. PET/CT also has the advantage of demonstrating metabolic activity in lymph nodes that do not demonstrate pathologic enlargement or abnormal enhancement on MRI, which did occur in a few instances in our study. Lastly, PET/CT can demonstrate reactive sclerosis and bony remodeling, which are not well evaluated by MRI. Although

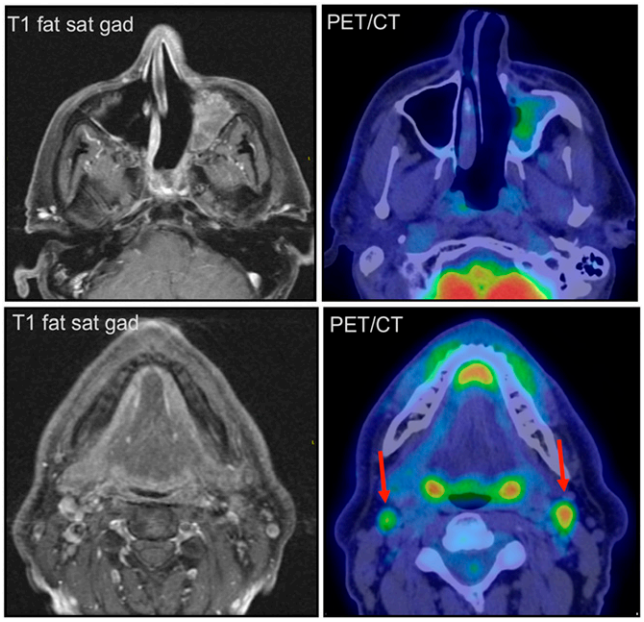

FIGURE 1. Patient 4 was a 46-y-old man with recurrent esthesioneuroblastoma. MRI and PET/CT demonstrate postoperative inflammation in the left maxillary sinus, whereas PET/CT demonstrates unsuspected bilateral cervical nodal metastasis (arrows). This finding prompted bilateral radical neck dissection, with pathologic confirmation of PET/CT findings.

not specific for tumor recurrence, this was a supportive finding in one of our patients.

Despite these advantages, PET/CT would have failed as a stand-alone modality in 5 (18%) of 28 patients. Three of these patients had intracranial metastases, which on PET/CT were impossible to distinguish from the high background ^{18}F-FDG accumulation in the brain. Although not unexpected, this problem does represent a shortcoming of using PET/CT to image a tumor that has a predilection for local, intracranial spread. Two patients had local esthesioneuroblastoma recurrence, which demonstrated significant gadolinium enhancement on MRI but only mild ^{18}F-FDG uptake on PET/CT and was interpreted incorrectly as inflammation.

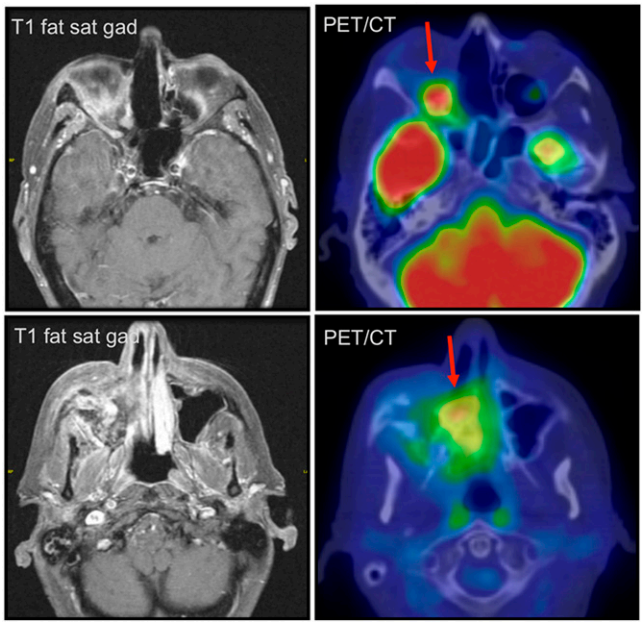

FIGURE 2. Patient 8 was a 70-y-old man with recurrent esthesioneuroblastoma. MRI was interpreted as showing only postoperative change, whereas PET/CT demonstrated extensive local recurrence, associated bony remodeling, and right orbital involvement (arrows). Patient opted for conservative management.

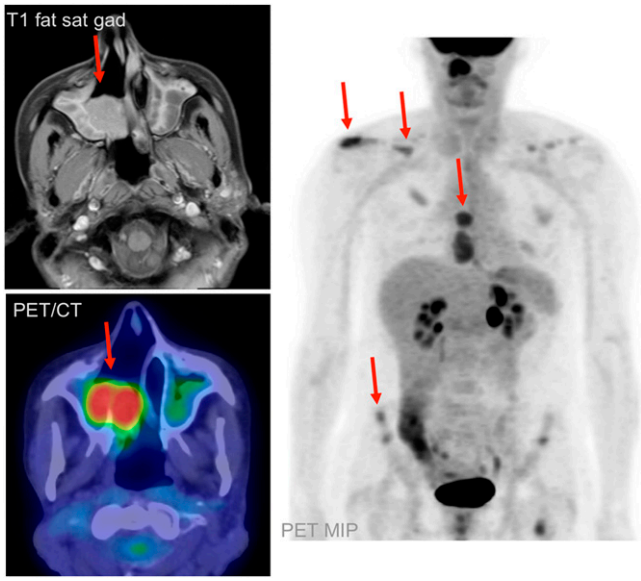

FIGURE 3. Patient 6 was a 44-y-old woman with recurrent esthesioneuroblastoma. MRI and PET/CT demonstrated local recurrence in right nasal cavity and maxillary sinus (arrow). PET/CT demonstrated unsuspected, extensive osseous metastases (arrows), altering management from possible surgical resection of local recurrence to salvage chemotherapy.

Given these findings, we suggest that the optimal imaging algorithm for the staging and restaging of esthesioneuroblastoma patients consists of combination PET/CT and contrast-enhanced MRI. Observationally, this seems to be the most common practice at our institution, although some heterogeneity exists among different clinicians and surgeons. Several studies have also demonstrated the utility of ^{68}Ga-DOTATOC PET in the evaluation of tumors expressing somatostatin receptor 2, including intracranial meningiomas (*17,18*). Because esthesioneuroblastoma has been shown to express somatostatin receptor 2 (*19*), ^{68}Ga-DOTATOC PET may have potential added benefit in esthesioneuroblastoma patients, particularly given that ^{18}F-FDG PET/CT performed poorly in patients with intracranial metastases in our study.

The primary tumors in our study population exhibited a wide range of ^{18}F-FDG accumulation, likely reflecting the broad variation in biologic behavior that has been observed in esthesioneuroblastoma patients (*2*). The calculated SUVmax measurements span from values typical of indolent neoplasms to intense activity seen in aggressive squamous

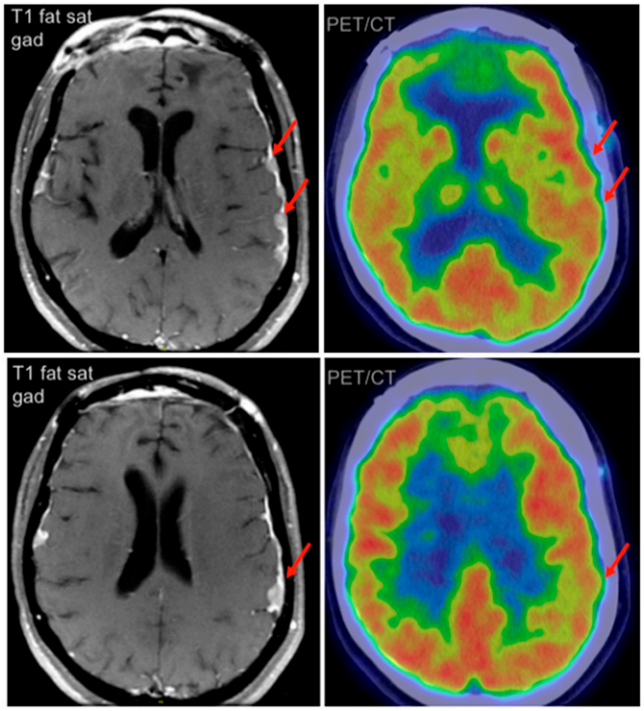

FIGURE 4. Patient 12 was a 47-y-old man with intracranial esthesioneuroblastoma metastases. MRI demonstrated nodular, enhancing metastases to left frontal and parietal dura, whereas PET/CT failed to demonstrate focal increase in ^{18}F-FDG activity in these regions. Metastatic esthesioneuroblastoma was confirmed by surgical biopsy.

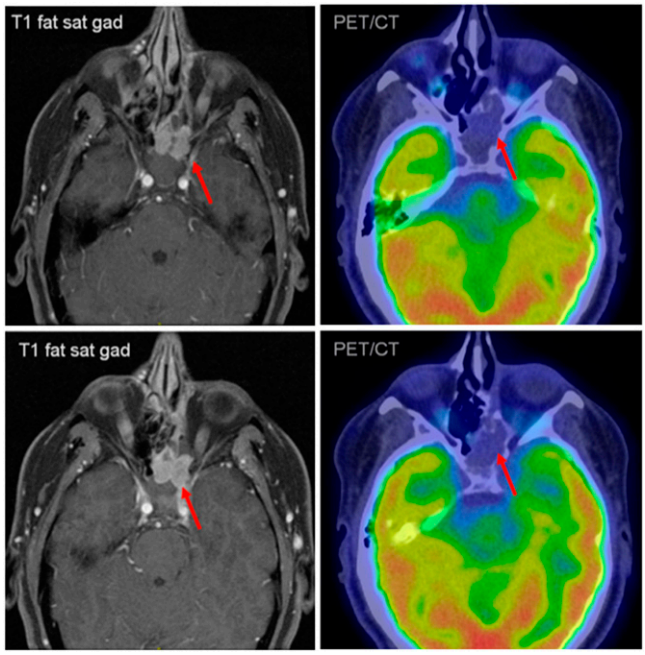

FIGURE 5. Patient 14 was a 40-y-old woman with locally recurrent esthesioneuroblastoma. MRI demonstrated local recurrence in left ethmoid and sphenoid sinuses, whereas PET/CT showed soft-tissue mass in this region without increased ^{18}F-FDG activity (arrows). Pathologic analysis of subsequently resected specimen demonstrated low-grade esthesioneuroblastoma.

cell head-and-neck malignancies. The recurrent and metastatic tumor foci also showed a wide range of metabolism. The minority with low ^{18}F-FDG uptake are prone to be overlooked as inflammation. Therefore, interpreters of PET/CT scans in patients with esthesioneuroblastoma need to be cognizant of the widely variable activity in the primary tumors, local recurrence, and metastatic disease.

Our study had several limitations. Although the standard PET/CT protocol at our institution uses low-dose, unenhanced CT, the addition of diagnostic CT with intravenous contrast material would likely result in detection of additional lesions and improved PET/CT performance, especially given that both primary esthesioneuroblastoma tumors and metastases show avid contrast enhancement (*8–10*). The role of PET/CT performed with full-dose contrast-enhanced CT in esthesioneuroblastoma patients should be evaluated, including its performance compared with and in conjunction with MRI. Another potential limitation of our methodology was the use of regions of interest instead of volumes of interest when calculating SUVmax. Although the use of regions of interest is our standard clinical practice, several studies have demonstrated that volumes of interest determined using isocontours based on fixed percentages result in greater SUVmax accuracy than those determined using manual regions of interest (*20–22*). Therefore, future efforts using automated volumes of interest may be preferable to our current technique.

Our study was also limited by its retrospective nature. Because of the tertiary nature of our institution, many patients underwent surgical resection of their primary tumor and received adjunctive treatment elsewhere, which led to incomplete clinical data, such as stage at initial presentation and primary tumor grade. This limitation also likely contributed to the larger than expected percentage of patients (86%) with advanced (Kadish C–D) disease and may have artificially elevated the prevalence (50%) of cervical metastases. Lastly, although to our knowledge this was the largest study to date, the number of patients included may have been too small to allow adequate assessment of a statistically significant correlation between tumor grade and SUVmax.

CONCLUSION

This study demonstrated that PET/CT is a useful adjunct to conventional imaging in the initial staging and restaging of esthesioneuroblastoma. PET/CT detects nodal and distant metastatic disease not demonstrated by dedicated MRI or CT of the head and neck. PET/CT identifies local recurrence hidden by treatment changes on conventional imaging. The use of PET/CT allows for improved patient management and therapy selection in esthesioneuroblastoma.

DISCLOSURE STATEMENT

The costs of publication of this article were defrayed in part by the payment of page charges. Therefore, and solely

to indicate this fact, this article is hereby marked "advertisement" in accordance with 18 USC section 1734.

ACKNOWLEDGMENT

No potential conflict of interest relevant to this article was reported.

REFERENCES

1. Broich G, Pagliari A, Ottaviani F. Esthesioneuroblastoma: a general review of the cases published since the discovery of the tumour in 1924. *Anticancer Res.* 1997;17:2683–2706.
2. Dulguerov P, Allal AS, Calcaterra TC. Esthesioneuroblastoma: a meta-analysis and review. *Lancet Oncol.* 2001;2:683–690.
3. Kadish S, Goodman M, Wang CC. Olfactory neuroblastoma: a clinical analysis of 17 cases. *Cancer.* 1976;37:1571–1576.
4. Jethanamest D, Morris LG, Sikora AG, Kutler DI. Esthesioneuroblastoma: a population-based analysis of survival and prognostic factors. *Arch Otolaryngol Head Neck Surg.* 2007;133:276–280.
5. Zanation AM, Ferlito A, Rinaldo A, et al. When, how and why to treat the neck in patients with esthesioneuroblastoma: a review. *Eur Arch Otorhinolaryngol.* 2010;267:1667–1671.
6. Morita A, Ebersold MJ, Olsen KD, Foote RL, Lewis JE, Quast LM. Esthesioneuroblastoma: prognosis and management. *Neurosurgery.* 1993;32: 706–714.
7. Dias FL, Sa GM, Lima RA, et al. Patterns of failure and outcome in esthesioneuroblastoma. *Arch Otolaryngol Head Neck Surg.* 2003;129:1186–1192.
8. Howell MC, Branstetter BF IV, Snyderman CH. Patterns of regional spread for esthesioneuroblastoma. *AJNR.* 2011;32:929–933.
9. Pickuth D, Heywang-Kobrunner SH. Imaging of recurrent esthesioneuroblastoma. *Br J Radiol.* 1999;72:1052–1057.
10. Yu T, Xu YK, Li L, et al. Esthesioneuroblastoma methods of intracranial extension: CT and MR imaging findings. *Neuroradiology.* 2009;51:841–850.
11. Zollinger LV, Wiggins RH III, Cornelius RS, Phillips CD. Retropharyngeal lymph node metastasis from esthesioneuroblastoma: a review of the therapeutic and prognostic implications. *AJNR.* 2008;29:1561–1563.
12. Nguyen BD, Roarke MC, Nelson KD, Chong BW. F-18 FDG PET/CT staging and posttherapeutic assessment of esthesioneuroblastoma. *Clin Nucl Med.* 2006;31:172–174.
13. Som PM, Curtin HD, Mancuso AA. Imaging-based nodal classification for evaluation of neck metastatic adenopathy. *AJR.* 2000;174:837–844.
14. Bradley PJ, Jones NS, Robertson I. Diagnosis and management of esthesioneuroblastoma. *Curr Opin Otolaryngol Head Neck Surg.* 2003;11:112–118.
15. Loy AH, Reibel JF, Read PW, et al. Esthesioneuroblastoma: continued follow-up of a single institution's experience. *Arch Otolaryngol Head Neck Surg.* 2006; 132:134–138.
16. Gore MR, Zanation AM. Salvage treatment of late neck metastasis in esthesioneuroblastoma: a meta-analysis. *Arch Otolaryngol Head Neck Surg.* 2009; 135:1030–1034.
17. Henze M, Dimitrakopoulou-Strauss A, Milker-Zabel S, et al. Characterization of ^{68}Ga-DOTA-D-Phe1-Tyr3-octreotide kinetics in patients with meningiomas. *J Nucl Med.* 2005;46:763–769.
18. Henze M, Schuhmacher J, Hipp P, et al. PET imaging of somatostatin receptors using [^{68}GA]DOTA-D-Phe1-Tyr3-octreotide: first results in patients with meningiomas. *J Nucl Med.* 2001;42:1053–1056.
19. Rostomily RC, Elias M, Deng M, et al. Clinical utility of somatostatin receptor scintigraphic imaging (OctreoScan) in esthesioneuroblastoma: a case study and survey of somatostatin receptor subtype expression. *Head Neck.* 2006;28: 305–312.
20. Boellaard R, Oyen WJ, Hoekstra CJ, et al. The Netherlands protocol for standardisation and quantification of FDG whole body PET studies in multi-centre trials. *Eur J Nucl Med Mol Imaging.* 2008;35:2320–2333.
21. Krause BJ, Beyer T, Bockisch A, et al. *Nuklearmedizin.* 2007;46:291–301.
22. Fletcher JW, Djulbegovic B, Soares HP, et al. Recommendations on the use of ^{18}F-FDG PET in oncology. *J Nucl Med.* 2008;49:480–508.